BIOLOGY OF REPRODUCTION **76,** 926–935 (2007)
Published online before print 21 February 2007.
DOI 10.1095/biolreprod.106.059766

Minireview

Vertebrate Yolk Complexes and the Functional Implications of Phosvitins and Other Subdomains in Vitellogenins[1]

Roderick Nigel Finn[2]

Department of Biology, University of Bergen, N-5020 Bergen, Norway

ABSTRACT

In nonplacental or nontrophotenic vertebrates, early development depends on the maternal provision of egg yolk, which is mainly derived from large multidomain vitellogenin (Vtg) precursors. To reveal the molecular nature of the protein pools in vertebrate oocytes, published data on the N-termini of yolk proteins has been mapped to the deduced primary structures of their parent Vtgs. The available evidence shows that the primary cleavage sites of Vtgs are conserved, whereas the cleavage products exist as multidomain variants in the yolk protein pool. The serine-rich phosvitin (Pv) domains are linearly related to the molecular masses of the lipovitellin heavy chain. The 3-D localization of Pv maps to the outer edges of the Vtg monomer, where it is proposed to form amphipathic structures that loop up over the lipid pocket. At this locus, it is proposed that Pv stabilizes the nascent Vtg while it receives its lipid cargo, thereby facilitating the hepatic loading and locking of lipid within the Vtg (C-sheet)-(A-sheet)-(LvL) cavity, and enhances its solubility following secretion to the circulating plasma. The C-terminal regions of Vtgs are homologous to human von Willebrand factor type D domains (Vwfd), which are conserved cysteine-rich molecules with homologous regions that are prevalent in Vtgs, lipophorins, mucins, integrins, and zonadhesins. Unlike human VWFD, lower vertebrate Vwfds do not contain RGD motifs, which are associated with extracellular matrix binding. Although its function in Vtg is unknown, the lubricant properties associated with mucins and the cell adhesion properties associated with integrins and zonadhesins implicate Vwfd in the genesis of hemostatic platelet aggregation. Similarly, the proteolytic inhibitory properties associated with the binding of factor VIII in humans suggest that Vwfd stabilizes Vtg during passage in the systemic circulation.

atherosclerosis, developmental biology, gametogenesis, hemostasis, lipoprotein, lipovitellin, oocyte development, von Willebrand factor

INTRODUCTION

Vitellogenins (Vtg) are large multidomain apolipoproteins that are the precursors of the major egg yolk proteins (Yps) in vertebrates and in most invertebrates [1–6]. In vertebrates, synthesis of Vtg occurs cotranslationally, primarily in the liver, as a result of a co-ordinated female-specific endocrine cascade that involves the brain, ovary, liver, and systemic circulation [7]. In vertebrates, a complete Vtg is composed of a signal peptide, a heavy chain lipovitellin (LvH), a phosvitin (Pv), a light chain lipovitellin (LvL), and a von Willebrand factor type D domain (Vwfd). In teleosts, the Vwfd is cleaved into the beta component (β′), and C-terminal coding region (CT). The β′ derives its name from earlier chromatographic studies of yolk proteins [8, 9]. After removal of the signal peptide, the mature vertebrate Vtg is linearly organized as a quadrapartite NH_2-(LvH-Pv-LvL-Vwfd)-COO^- monomer, while the teleost Vtg is organized as a pentapartite NH_2-(LvH-Pv-LvL-β′-CT)-COO^- monomer (Fig. 1).

All vertebrate Vtgs are posttranslationally glycosylated and phosphorylated in the endoplasmic reticulum (ER) and Golgi complex before being tagged for export, and are secreted to the circulating plasma as homodimeric lipoprotein complexes. During passage through the ovary, specific receptors (Vtgr), which are anchored in the oocyte plasma membrane, bind Vtg and become internalized with their Vtg ligands via clathrin-mediated endocytosis [10, 11]. Recent data suggest that receptor complexes that lack AP-2 adapters preferentially target internalized cargo, such as low-density lipid particles, to a population of degradative endosomes [12–15]. It is also known that internalized vesicles that contain the related very high-density Vtg are rapidly sorted to early endosomes in the oocyte where they are acidified due to the action of ATP-dependent V-class proton pumps [4, 10, 16–19]. The acidification activates cathepsin D (CatD), which cleaves Vtg into its constituent Yps [20–25]. In vertebrates, this is known as the primary cleavage event of Vtg, and it yields lipovitellins (Lv), Pv, and β′ (reviewed in [26, 27].

In a recent study of the structure and disassembly of Vtgs and Yps in a marine pelagophil teleost [5], it has been suggested that the Pv domains remain covalently attached to the LvL of one paralogue (HhvtgAa) but to the C-terminal subunit (LvHc-Ab) of the other paralogue (HhvtgAb). Due to the multiplicity of the Vtg family [5, 6, 28–45], it has proven challenging to establish the precursor-product relationships between Vtgs and Yps based on their physical, chemical or antigenic properties. Given the increased information on the deduced primary structures of the parent Vtgs together with the N-terminal peptide data on the derivative Yps, it is now possible to ascertain whether vertebrate Vtgs are indeed cleaved into their constituent Lv, Pv, and β′ Yps. Similarly, the primary structural data can be related to the growing number of resolved 3-D models, providing new insights into the cellular functions of the Pv and Vwfd subdomains. In the

[1]Supported in part by the Research Council of Norway and the University of Bergen.
[2]Correspondence: FAX: 47 55 589667; e-mail: nigel.finn@bio.uib.no

Received: 23 December 2006.
First decision: 26 January 2007.
Accepted: 20 February 2007.

ISSN: 0006-3363. http://www.biolreprod.org

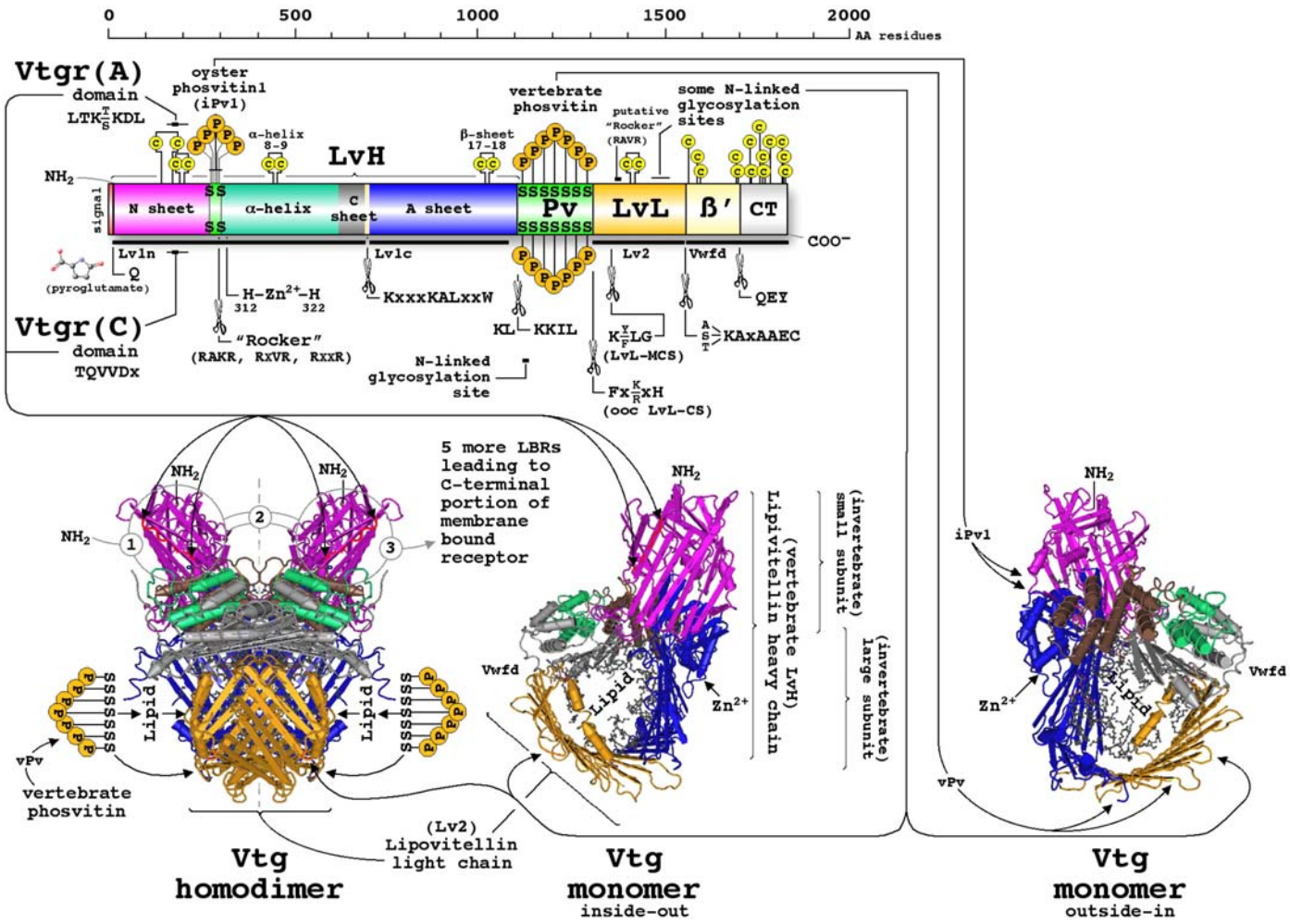

FIG. 1. Linear scale representation of the pentapartite NH_2-(LvH-Pv-LvL-β′-CT)-COO^- subdomain structure of a complete teleost vitellogenin (Vtg), showing the salient features mapped to the 3-D structures of a lamprey lipovitellin homodimer and rotated monomer [64, 69]. The precise Vtg subdomain maps were obtained from an alignment of vertebrate vitellogenins [6]. A short signal peptide is shown that leads to the LvH N-terminus, which in vertebrates appears to be a pyroglutamate. Consensus sequences of the subdomain cleavage sites are shown along the length of the Vtg bar. Most of these sites are recognized by cathepsin D. However, the LvL may be processed at either the N-terminal oocyte LvL cleavage site (ooc LvL-CS) or a second more C-terminal egg LvL maturational cleavage site (LvL-MCS). In the latter case, cathepsin B or cathepsin L cleaves the molecule during oocyte maturation in teleosts [23]. A conserved Asn-glycosylation site is identified near the N-terminus of the vertebrate Pv domain. Cysteine (Cys) residues are shown in yellow circles, and are linked where disulfide bridges are known to exist. Phosphates, schematically shown in orange circles, are mostly phosphorylated to Ser (S) residues in the Pv domains [61]. The 3-D structure was assembled from snapshots of lipovitellin worms rendered using Cn3D [119]. The colors of the LvH (N-sheet)-(α-helix)-(C-sheet)-(A-sheet) subdomains and the LvL domain match the default domain colors of the protein data bank model when rendered in Cn3D. The vertebrate Pv (vPv) domain (not modeled) is drawn at the outer edges of the homodimeric Vtg structure to illustrate its putative function. The vitellogenin receptor (Vtgr: A- and C-type Vtgs) minimal interaction domains were identified after Li et al. [120] and mapped to an exposed β-sheet of the LvH N-sheet between a tetrad of fully conserved Cys residues. These Cys residues form disulfide bridges [64] that stabilize the conformation of the N-sheet by linking two small β-sheets and an otherwise disordered loop that interacts with the C-sheet. The three most-N-terminal ligand-binding repeats (LBRs) of the Vtgr monomer (labeled 1, 2, and 3) are superimposed on the exposed β-sheets of the Vtg homodimer. The putative binding site for Zn^{2+} [64] is shown between two highly conserved His residues. The first oyster phosvitin (iPv1) is mapped to illustrate its primary locus in the linear model. Shown is the conserved putative invertebrate furin cleavage site (RAKR, RxVR, RxxR; pronounced "Rocker" in a Rastafarian dialect), which separates the small subunit from the large subunit in invertebrate Vtgs. Although iPv1 is not present in vertebrate Vtgs, a conserved putative (Rocker) furin cleavage site exists in the LvL domains of vertebrates.

present review, the new Vtg gene nomenclature of Finn and Kristoffersen [6] is used.

YOLK COMPLEXES

Amphibia

For amphibians, the Pv domains have been characterized for African clawed frog, and depending on the study, have reported molecular masses of 16–19 kDa [46], 25 kDa [47], or 31 kDa [48]. In addition, the N-termini of the LvL domains from VtgABa1, VtgABa2, and VtgABb1 have been identified [49]. These N-termini precisely match the cleavage sites of LvL-Aa and LvL-Ab revealed in the recent study on Atlantic halibut [5] and the fully conserved Phe in the alignment of Finn and Kristoffersen [6]. Since the LvH domains have been independently estimated at 120 kDa [48], which matches the molecular mass predicted from the sequenced genes [47, 50], the reported molecular mass of Pv should match the molecular masses of 23.2 kDa and 23.7 kDa calculated for VtgABa2 and VtgABb1, respectively (Fig. 2). The data of Yoshitome et al. [47] are a good match, while the data of Ohlendorf et al. [46] indicate that smaller cleavage variants may exist. Thus, in

FIG. 2. Predicted molecular masses (kDa) of vertebrate vitellogenins, subdomains, and conjugates. Each subdomain is identified from conserved cleavage sites [5, 6]. The molecular masses of the oocyte LvL-CS conjugates are predicted when the LvL subdomain is cleaved at the conserved $Fx^{K}/_{R}xH$ cleavage site, while the molecular masses of the egg LvL-MCS conjugates are predicted when the LvL subdomain is cleaved after Gly at the conserved $K^{Y}/_{F}LG$ maturational cleavage site (see Fig. 1). The reclassified Vtg gene homologue nomenclature [6] is given and compared to the earlier nomenclature. Vtg, vitellogenin; LvH, lipovitellin heavy chain; Pv, phosvitin; LvL, lipovitellin light chain; β', beta' component; CT, C-terminal coding region; CS, cleavage site; MCS, maturational cleavage site.

							Vg sub-domains						oocyte LvL-CS conjugates								LvL-MCS conjugates		
	Accession Number (NCBI \ Ensembl)	Order	Animal	Species	Previous homologue name	Reclassified Vitellogenin homologue	LvH	Pv	LvL	β'	CT	Full Vtg	LvH-Pv	LvH-Pv-LvL	LvH-Pv-LvL-β'	LvH-LvL	Pv-LvL	Pv-LvL-β'	Pv-LvL-β'-CT	β'-CT	LvH-Pv	Pv	LvL
1	NEWSINFRUP00000179080	Tetraodontiformes	Torafugu Pufferfish	*Takifugu rubripes*	novel	VtgAb	116.3	22.3	24.8	17.0	13.5	**193.9**	138.6	163.4	180.4	-	47.1	64.1	77.6	30.5	142.4	26.1	21.0
2	NEWSINFRUP00000131263	Tetraodontiformes	Torafugu Pufferfish	*Takifugu rubripes*	novel	VtgC	115.2	0.8	18.1	-	-	**134.1**	116.0	134.1	-	133.3	18.9	-	-	-	116.4	1.2	17.8
3	hhvtgAa	Pleuronectiformes	Atlantic halibut	*Hippoglossus hippoglossus*	novel	VtgAa	114.5	6.5	25.5	17.1	13.1	**176.7**	121.0	146.5	163.6	-	32.0	49.1	62.2	30.2	125.3	10.8	21.0
4	hhvtgAb	Pleuronectiformes	Atlantic halibut	*Hippoglossus hippoglossus*	novel	VtgAb	114.4	7.4	25.9	17.3	13.6	**178.6**	121.8	147.7	165.0	-	33.3	50.6	64.2	30.9	125.8	11.4	21.9
5	AB181833	Pleuronectiformes	Barfin Flounder	*Verasper moseri*	VgA	VtgAa	114.5	5.9	25.7	17.1	13.1	**176.3**	120.4	146.1	163.2	-	31.6	48.7	61.8	30.2	124.9	10.4	21.3
6	AB181834	Pleuronectiformes	Barfin Flounder	*Verasper moseri*	VgB	VtgAb	114.5	8.1	25.9	17.3	13.6	**179.4**	122.6	148.5	165.8	-	34.0	51.3	64.9	30.9	126.6	12.1	21.9
7	AB181838	Perciformes	Red Seabream	*Pagrus major*	VgA	VtgAa	115.3	14.0	25.4	17.1	13.5	**185.3**	129.3	154.7	171.8	-	39.4	56.5	70.0	30.6	133.4	18.1	21.3
8	AB181839	Perciformes	Red Seabream	*Pagrus major*	VgB	VtgAb	116.4	13.3	26.1	17.2	13.7	**186.7**	129.7	155.8	173.0	-	39.4	56.6	70.3	30.9	133.8	17.4	22.1
9	AB181840	Perciformes	Red Seabream	*Pagrus major*	VgC	VtgC	115.4	2.8	22.0	-	-	**140.2**	118.2	140.2	-	137.4	24.8	-	-	-	118.6	3.2	21.7
10	AB081299	Perciformes	Japanese silago	*Sillago japonica*	Vg	VtgAa	115.3	13.0	25.6	17.3	13.0	**184.2**	128.3	153.9	171.2	-	38.6	55.9	68.9	30.3	132.7	17.4	21.2
11	AB088473	Perciformes	Japanese common Goby	*Acanthogobius flavimanus*	Vg-530	VtgAa	116.5	12.1	25.7	17.0	12.9	**184.2**	128.6	154.3	171.3	-	37.8	54.8	67.7	29.9	132.4	15.9	21.9
12	AB088474	Perciformes	Japanese common Goby	*Acanthogobius flavimanus*	Vg-320	VtgC	117.2	1.7	20.0	-	-	**138.9**	118.9	138.9	-	137.2	21.7	-	-	-	119.4	2.2	19.5
13	AF017250	Perciformes	Blue tilapia	*Oreochromis aureus*	Vtg1	VtgAb	116.4	20.9	25.9	16.9	13.5	**193.6**	137.3	163.2	180.1	-	46.8	63.7	77.2	30.4	141.4	25.0	21.7
14	ENSGACP00000012923	Gasterosteiformes	3-spined stickleback	*Gasterosteus aculeatus*	novel	VtgAa	115.6	8.1	25.4	17.2	13.7	**180.0**	123.7	149.1	166.3	-	33.5	50.7	64.4	30.9	127.9	12.3	21.3
15	ENSGACP00000012842	Gasterosteiformes	3-spined stickleback	*Gasterosteus aculeatus*	novel	VtgAb	64.1	12.1	26.4	4.8	-	**107.4**	76.2	102.6	-	-	38.5	43.3	43.3	-	16.3	16.3	22.2
16	ENSGACP00000012536	Gasterosteiformes	3-spined stickleback	*Gasterosteus aculeatus*	novel	VtgC	115.7	2.4	22.6	-	-	**140.7**	118.1	140.7	-	138.3	25.0	-	-	-	119.2	3.5	21.5
17	AB181835	Atheriniformes	Mosquitofish	*Gambusia affinis*	VgA	VtgAa	117.7	13.1	25.6	17.4	12.9	**186.7**	130.8	156.4	173.8	-	38.7	56.1	69.0	30.3	134.8	17.1	21.6
18	AB181836	Atheriniformes	Mosquitofish	*Gambusia affinis*	VgB	VtgAb	116.7	9.8	27.1	17.2	13.8	**184.6**	126.5	153.6	170.8	-	36.9	54.1	67.9	31.0	130.7	14.0	22.9
19	AB181837	Atheriniformes	Mosquitofish	*Gambusia affinis*	VgC	VtgC	115.4	2.3	21.6	-	-	**139.3**	117.7	139.3	-	137.0	23.9	-	-	-	118.0	2.6	21.3
20	AB064320	Beloniformes	Medaka	*Oryzias latipes*	Ol-vit1	VtgAa	115.9	12.4	25.6	17.3	13.1	**184.3**	128.3	153.9	171.2	-	38.0	55.3	68.4	30.4	132.4	16.5	21.5
21	AB074891	Beloniformes	Medaka	*Oryzias latipes*	VgII	VtgAb	116.9	14.8	26.2	17.2	13.8	**188.9**	131.7	157.9	175.1	-	41.0	58.2	72.0	31.0	136.0	19.1	21.9
22	ENSORLP00000008173	Beloniformes	Medaka	*Oryzias latipes*	novel	VtgC	114.5	0.3	21.0	-	-	**135.8**	114.8	135.8	-	135.5	21.3	-	-	-	115.3	0.8	20.5
23	U07055	Cyprinodontiformes	Common Mummichog	*Fundulus heteroclitus*	VtgI	VtgAa	117.1	14.6	24.7	17.2	12.7	**186.3**	131.7	156.4	173.6	-	39.3	56.5	69.2	29.9	135.0	17.9	21.5
24	FHU70826	Cyprinodontiformes	Common Mummichog	*Fundulus heteroclitus*	VtgII	VtgAb	116.4	10.8	26.6	17.1	13.6	**184.5**	127.2	153.8	170.9	-	37.4	54.5	68.1	30.7	131.4	15.0	22.4
25	AY279214	Cyprinodontiformes	Mangrove killifish	*Rivulus marmoratus*	Vtg	VtgAa	117.1	15.3	25.3	17.2	12.3	**187.2**	132.4	157.7	174.9	-	40.6	57.8	70.1	29.5	135.9	18.8	21.8
26	AF284035	Gadiformes	Haddock	*Melanogrammus aeglefinus*	VtgA	VtgAa	116.1	8.8	25.4	17.2	13.6	**181.1**	124.9	150.3	167.5	-	34.2	51.4	65.0	30.8	128.9	12.8	21.4
27	AF284034	Gadiformes	Haddock	*Melanogrammus aeglefinus*	VtgB	VtgAb	115.2	5.7	25.8	16.8	13.6	**177.1**	120.9	146.7	163.5	-	31.5	48.3	61.9	30.4	124.9	9.7	21.8
28	X92804	Salmoniformes	Rainbow Trout	*Oncorhynchus mykiss*	VtgA	VtgAsa	116.5	7.1	26.9	17.4	13.7	**181.6**	123.6	150.5	167.9	-	34.0	51.4	65.1	31.1	127.7	11.2	22.9
29	AF414432	Ostariophysi	Common Carp	*Cyprinus carpio*	Vg	VtgAo1	114.0	6.2	26.3	0.4	-	**146.9**	120.2	146.5	-	-	32.5	32.9	-	-	124.5	10.5	21.9
30	AB106873	Ostariophysi	Common Carp	*Cyprinus carpio*	Vg	VtgAo2	114.3	5.7	26.2	17.3	13.3	**176.8**	120.0	146.2	163.5	-	31.9	49.2	62.5	30.6	124.4	10.1	21.8
31	AF130354	Ostariophysi	Fathead minnow	*Pimephales promelas*	Vg	VtgAo1	112.9	5.5	26.0	0.4	-	**144.8**	118.4	144.4	-	-	31.5	31.9	-	-	122.6	9.7	21.7
32	AF406784	Ostariophysi	Zebrafish	*Danio rerio*	Vg1	VtgAo1	114.4	6.9	26.3	0.4	-	**148.0**	121.3	147.6	-	-	33.2	33.6	-	-	125.8	11.4	21.9
33	ENSDART00000044869	Ostariophysi	Zebrafish	*Danio rerio*	Vg2	VtgAo2	115.2	6.9	30.9	17.1	13.2	**183.3**	122.1	153.0	170.1	-	37.8	54.9	68.1	30.3	130.5	15.3	22.3
34	AF254638	Ostariophysi	Zebrafish	*Danio rerio*	Vg3	VtgC	114.9	2.3	21.2	-	-	**138.4**	117.2	138.4	-	136.1	23.5	-	-	-	117.6	2.7	20.7
35	*AY423444*	Anguilliformes	Japanese eel	*Anguilla japonica*	VTG2	VtgAe1	116.5	12.4	28.2	17.1	13.6	**187.8**	128.9	157.1	174.2	-	40.6	57.7	71.3	30.7	136.7	20.2	20.4
36	AY423445	Anguilliformes	Japanese eel	*Anguilla japonica*	VTG1	VtgAe2	113.8	12.8	28.1	17.1	13.6	**185.4**	126.6	154.7	171.8	-	40.9	58.0	71.6	30.7	134.3	20.5	20.4
37	AY775788	Anguilliformes	Japanese eel	*Anguilla japonica*	Vtg	VtgAe3	114.3	12.9	28.2	17.1	13.6	**186.1**	127.2	155.4	172.5	-	41.1	58.2	71.8	30.7	135.0	20.7	20.4
38	AB185334	Anguilliformes	Japanese conger eel	*Conger myriaster*	vtg	VtgAe3	114.3	6.3	26.9	17.1	13.5	**178.1**	120.6	147.5	164.6	-	33.2	50.3	63.8	30.6	126.9	12.6	20.5
39	U00455	Chondrostei	White sturgeon	*Acipenser transmontanus*	vitellogenin	VtgAB	118.9	18.3	26.8	17.3	4.1	**185.4**	137.2	164.0	181.3	-	45.1	62.4	66.5	21.4	131.5	12.6	22.1
40	D89547	Aves	Chicken	*Gallus gallus*	Vit1	VtgAB1	119.0	27.9	31.5	17.1	13.6	**209.1**	146.9	178.4	195.5	-	59.4	76.5	90.1	30.7	156.5	37.5	21.9
41	NM_001031276	Aves	Chicken	*Gallus gallus*	Vit2	VtgAB2	120.0	25.9	27.2	16.7	13.6	**203.4**	145.9	173.1	189.8	-	53.1	69.8	83.4	30.3	150.8	30.8	22.3
42	ENSGALP00000002886	Aves	Chicken	*Gallus gallus*	novel	VtgAB3	116.6	11.4	26.9	17.3	13.4	**185.6**	128.0	154.9	172.2	-	38.3	55.6	69.0	30.7	132.5	15.9	22.4
43	AY045719	Aves	Herring gull	*Larus argentatus*	vitellogenin	VtgAB	119.1	23.5	27.2	17.1	13.4	**200.3**	142.6	169.8	186.9	-	50.7	67.8	81.2	30.5	147.4	28.3	22.3
44	M18061	Amphibia	African clawed frog	*Xenopus laevis*	vtgA2	VtgABa2	118.8	23.2	27.2	17.4	13.2	**199.8**	142.0	169.2	186.6	-	50.4	67.8	81.0	30.6	146.4	27.6	22.8
45	AB092605	Amphibia	African clawed frog	*Xenopus laevis*	vtgB1	VtgABb1	120.1	23.7	27.5	17.3	13.4	**202.0**	143.8	171.3	188.6	-	51.2	68.5	81.9	30.7	148.6	28.5	22.6
46	M88749	Petromyzontiformes	Silver lamprey	*Ichthyomyzon unicuspus*	vitellogenin	VtgABCD	122.1	19.1	27.8	16.4	12.8	**198.2**	141.2	169.0	185.4	-	46.9	63.3	76.1	29.2	146.4	24.3	22.7
						Mean	116.2	11.2	25.7	15.5	13.1	**176.7**	127.4	153.1	173.8	136.4	37.0	55.1	69.7	30.2	128.8	15.2	21.6
						± SD	1.9	7.1	2.5	4.9	1.6	**20.9**	8.6	10.3	8.4	1.6	8.8	9.5	8.1	1.6	19.5	8.3	0.9

amphibians, Vtgs seem to be processed into separate Lv and Pv components. However, the situation in birds and fishes is more complex.

Birds

The chicken carries multiple copies of Vtg, which have previously been chronologically classified as Vtg1, Vtg2, and Vtg3 [51–54]. These genes have recently been reclassified phylogenetically as VtgAB1, VtgAB2, and VtgAB3, respectively [6]. Within the chicken Vtg genes, up to five Pv variants exist. Smaller phosvettes, which range in size from 13 kDa to 18 kDa, and 'full' Pvs, which range in size from 28 kDa to 50 kDa, have been reported [5, 55–60]. The predicted molecular masses of the chicken Pv proteins cleaved between the conserved KKIL site and the conserved HhvtgAa Phe_{1131} putative CatD cleavage site should be 27.9 kDa, 25.9 kDa, and 11.8 kDa for VtgAB1, VtgAB2, and VtgAB3, respectively (Fig. 2). However, N-terminal data for the major avian Pvs reported for chicken and ducks [61] indicate that the chicken VtgAB2 Pv N-terminus is AEFGTEP, which lies 31 amino acids (aa) downstream of the KKIL motif. Thus, the predicted molecular mass of chicken VtgAB2 Pv would be even smaller at 22.3 kDa. While the molecular mass of VtgAB3 Pv may explain some of the phosvette reports, this value is clearly at the lower end of the observed values. Similarly, only the lower value of 28 kDa for full Pvs corroborates the calculated molecular masses of the Pv proteins. When Groche et al. [62] subjected chicken LvLs to Edman degradation they observed multiple aa signals from the third cycle onwards, so they were unable to identify definitively the N-terminus of LvL. Thus, it is not possible to verify that the conserved HhvtgAa Phe_{1131} is in fact the N-terminus of chicken LvLs, despite the conserved Phe being located in this motif in each of the chicken Vtgs.

In the recent study on Atlantic halibut [5], it was noted that during the maturational proteolysis of the Vtg paralogues that the LvLs were N-terminally truncated, by 40 aa in LvL-Aa and by 35 aa in LvL-Ab, to a position two aa downstream of a highly conserved Tyr/Phe (Tyr_{1168}, HhvtgAa; Tyr_{1173}, HhvtgAb). This precise pattern of maturational processing also occurs in the barfin flounder [30], in the common mummichog [29], and in all three expressed Vtgs of red seabream [44]. Therefore, this site is termed the oocyte maturational LvL N-terminal cleavage site (LvL-MCS). It is the putative recognition site for CatB and/or CatL. An exact match for this site (FLGDIK) was identified in tryptic digests of the 30-kDa chicken VtgAB2 LvL [62].

Given that the LvL-MCS is the N-terminal processing site for chicken LvLs, the predicted molecular masses of VtgAB1, VtgAB2, and VtgAB3 should be 37.5 kDa, 30.8 kDa, and 15.9 kDa, respectively (Fig. 2). These latter values resemble the molecular masses observed for the Pvs [56–60], but still fall short of the higher than 40 kDa molecular masses of the Pvs, including the 50-kDa major band, observed by Finn [5]. However, the molecular masses derived from SDS-PAGE have been reported as 30 kDa for the chicken LvLs [2, 62], and as ~32 kDa for CatD-processed Lv in both chicken and Japanese quail [59]. The predicted molecular masses of the LvLs cleaved at the LvL-CS are 31.5 kDa, 27.2 kDa, and 26.9 kDa for VtgAB1, VtgAB2, and VtgAB3, respectively, while the predicted molecular masses of the LvLs cleaved C-terminally at the conserved Tyr/Phe (LvL-MCS) are 21.9 kDa, 22.3 kDa, and 22.4 kDa for VtgAB1, VtgAB2, and VtgAB3, respectively (Fig. 2). Unlike Pv, LvL is not known to show anomalous behavior in SDS-PAGE, and thus the latter molecular mass values for LvLs are significantly lower than predicted, while the former closely match the observed molecular masses for LvLs [2, 59, 62]. This suggests that the LvL-CS identified by Finn [5] is indeed the recognition site for CatD and the N-termini of chicken LvLs, as previously shown for amphibians and presently shown for teleosts (see below). The predicted Pv-LvL conjugates of the major and minor chicken Vtgs (VtgAB1 and VtgAB2) processed at the LvL-CS are 59.4 kDa and 53.1 kDa, respectively (Fig. 2). These conjugates closely match the higher in-gel molecular masses observed for full Pvs [5, 57, 59]. From this analysis, it can be inferred that the chicken Pvs with molecular masses greater than 25 kDa have Lv fragments attached to them.

Teleosts

It is only recently that sufficient N-terminal sequence data for Vtg-derived Yps in fish have become available. The Vtgs of barfin flounder and red seabream are cleaved at the fully conserved LvL-CS Phe (HhvtgAa Phe_{1131}), establishing the N-termini of the LvLs in these species [30, 44]. Data for Japanese common goby, which has two Vtg forms, a VtgAa type (reported as Vg-530) and a VtgC type (reported as Vg-320) [38], show that the VtgAa LvL is also cleaved at the fully conserved LvL-CS, and therefore, the LvL N-terminus is identical to that of the Atlantic halibut [5]. The VtgC form is not processed and remains as an LvH-LvL conjugate in the oocyte yolk [38]. A similar observation has been made for Mozambique tilapia [63]. Yolk proteolysis during oocyte maturation has not yet been studied in the Japanese common goby or Mozambique tilapia. In a similar study on the ovoviviparous mosquitofish, Sawaguchi et al. [42, 43] identified three forms of Vtg, which were previously classified as VgA, VgB, and VgC but are reclassified as VtgAa, VtgAb, and VtgC, respectively [6]. Surprisingly, despite having the KKIL site and the LvL-CS, the VtgAa form is not cleaved into Lv and Pv, but remains as conjugates that range from full Vtg (LvH-Pv-LvL-β′-CT) to Pv-LvL, while in the VtgAb form, only LvH was identified. In the VtgC form, which lacks Pv and the fully conserved Phe (HhvtgAa Phe_{1131}) of the complete Vtgs, unprocessed LvH-LvL, cleaved LvH, and LvL proteins can be found [42]. In the only other species (the common mummichog) for which Vtg-Yp sequence maps exist, LaFleur et al. [29] have revealed that the two forms of Vtg, reported earlier as VtgI and VtgII, [28] but now reclassified as VtgAa, and VtgAb, respectively [6], are differentially processed. In the VtgAa form, the LvH-Aa form exists as a complete 122-kDa protein (Yp122) and an N-terminal 103-kDa fragment (Yp103 = LvHn-Aa). The C-terminal fragment of the LvH-Aa is a 19-kDa protein (Yp19 = LvHc-Aa), which is cleaved only four aa upstream of the LvHc-Aa cleavage site in Atlantic halibut [5, 29]. In the VtgAb form, only the N-terminal fragment LvHn with a molecular mass of 69 kDa (Yp69) has been identified [29]. This is very close to the molecular mass of the lamprey Lv1n domain (67 kDa), which is cleaved at the end of the C-sheet [64], and it is suggested that the mummichog LvHn-Ab is homologous to this peptide fragment. Interestingly, peptides of the same molecular mass appear temporarily as Yp8 during the maturational proteolytic events in halibut [5, 65]. The N-terminus of the mummichog LvL-Aa identified by LaFleur et al. [29] is located at the LvL-CS, but with a molecular mass of 45 kDa it is almost twice the size of the predicted LvL-Aa protein of 24.7 kDa (Fig. 2), and must therefore be covalently linked to the β′ and much of the CT, which together represent the Vwfd domain. It is reasonable to make this assumption, since LaFleur et al. [29] have identified the β′ component as a 26-kDa protein (Yp26).

Class / Order / Animal	Paralogue VtgAa Vtg M_r (kDa) [ratio]	Yp M_r (kDa)	Major/minor	oocyte	OV egg	Conjugate	Paralogue VtgAb Vtg M_r (kDa) [ratio]	Yp M_r (kDa)	Major/minor	oocyte	OV egg	Conjugate	Homologue VtgC Vtg M_r (kDa) [ratio]	Yp M_r (kDa)	Major/minor	oocyte	OV egg	Conjugate	Source
Acanthopterygii																			
Pleuronectiformes																			
Atlantic halibut	178	110	M	√	x	LvH	180	92	M	√	√	LvHn							[1]
(Hippoglosusus hippoglossus)	[1]						[:3]	12	M	√	x	LvHc-Pv							
								9	M	√	√	LvHc							
		30	M	√	x	Pv-LvL		30	m	√	x	Pv-LvL							
		28	M	√	√	LvL		27	M	√	√	LvL							
		17	M	√	x	ß´		17	M	√	x	ß´							
Barfin flounder	168	107	M	√	x	LvH	175	102	m	√	x	LvH							[30,31]
(Verasper moseri)	[2]						[:3]	94	M	√	√	LvHn							
		42	M	√	x	Pv-LvL		28	M	√	x	Pv-LvL							
		30	M	√	√	LvL		27	M	√	√	LvL							
		17	M	√	x	ß´		17	M	√	x	ß´							
		18	M	√	x	CT		18	M	√	x	CT							
Perciformes																			
Japanese common goby	178	157	M	√	na	LvH-Pv-LvL							127	127	M	√	na	LvH-LvL	[37,38]
(Acanthogobius flavimanus)	[5]	17	M	√	na	ß´							[:1]						
Red sea bream	182	182	M	√	x	LvH-Pv-LvL-ß´-CT	182	182	M	√	x	LvH-Pv-LvL-ß´-CT	137	137	M	√	x	LvH-LvL	[44]
(Pagrus major)	[na]						[na]	160	M	√	x	LvH-Pv-LvL	[na]	70	M	√	√	LvHn	
								140	M	√	x	LvH-Pv		41	M	√	√	LvHc-LvL	
		110	M	√	x	LvH		110	M	√	√	LvH		28	M	√	un	LvL	
		61	M	√	x	Pv-LvL		23	M	√	x	$Pv\text{-}LvL_{start}$							
		26	M	√	√	LvL		29	M	√	√	LvL							
		17	M	√	x	ß´		18	M	√	x	ß´							
Cyprinodontiformes																			
Common mummichog	188	122	M	√	x	LvH	185	69	M	√	√	LvHn							[29]
(Fundulus heteroclitus)	[10]	103	M	√	√	LvHn	[:1]												
		19	M	√	√	$LvHc\text{-}Pv_{start}$													
		45	M	√	√	LvL-ß´-CT													
		26	m	√	√	ß´													
Atheriniformes																			
Mosquitofish	195	195	m	√	na	LvH-Pv-LvL-ß´-CT	195	126	M	√	na	LvH	142	142	m	√	na	LvH-LvL	[42,43]
(Gambusia affinis)	[1]	175	M	√	na	LvH-Pv-LvL	[:1]						[:0.1]	112	M	√	na	LvH	
		66	m	√	na	Pv-LvL								33	M	√	na	LvL	
		21	M	√	na	ß´													
Paracanthopterygii																			
Gadiformes																			
Haddock	182	112	M	√	x	LvH	179	111	M	√	√	LvH							[33]
(Melanogrammus aeglefinus)	[1]						[:1]												
Hyperoartia																			
Cephalospidomorphi																			
Silver lamprey	200	66.8	M	√	na	LvHn													[64]
(Ichthyomyzon unicuspis)		40.8	M	√	na	LvHc													
		35.2	M	√	na	LvL													

FIG. 3. Vitellogenin (Vtg)-derived structural conjugates of yolk proteins (Yp) in fish species. Only species that have their Vtg cDNA independently corroborated by N-terminal data or mass-spectrometry of the Yp are shown. Precursor molecular masses include the signal peptide. Proteins are categorized as major (M) or minor (m) according to their in-gel staining intensity. The presence or absence of the conjugates in the oocyte and/or ovulated egg (OV egg) is indicated by √ or x, respectively. Specifically for OV eggs, the √ designation indicates the maturational survival of all or part of the protein. The numbers in square parentheses represent the molar expression ratios between the Vtg forms (paralogue, homologue) of each species (na, not investigated; un, undetected).

Interestingly, during oocyte maturation in the mummichog, the (LvL-β′-CT)-Aa Yp45 is N-terminally processed to a 42-kDa (LvL-β′-CT)-Aa Yp42 protein in precisely the same manner as has been described for Atlantic halibut and other species at the conserved LvL-MCS [5]. A summary of these findings is provided in Figure 3, where it is shown that the primary CatD cleavage products of Vtg in fish exist as multidomain variants rather than separate Pvs and Lvs, as is commonly thought.

PHOSVITIN FUNCTIONS

Earlier hypotheses regarding the functional significance of the Pv domains arose from observations that the domain was present only in vertebrates, with the largest tracts occurring in terrestrial vertebrates [2]. These observations gave rise to the length-evolution relationship and the notion that the P_i and Ca^{2+} ported by the Pv domains are used for bone formation. The latter notion is well established in the literature [27]. The discovery that agnathans and teleosts also contain Pv domains that are equal in size to those of the terrestrial vertebrates [66, 67] shed doubt on the length-evolution idea. Similarly, the observation that insects have, albeit unrelated, polyserine tracts [3, 4, 68] raises doubts about the bone formation hypothesis.

In a recent study, Finn and Kristoffersen [6] have proposed that the origin of the first of the two insect Pvs (iPv1; see Fig. 1) and the single vertebrate Pv domain (vPv) can be traced back to the Mollusca (Pacific oyster). This indicates that Pv has been present in Vtgs at least since the Tommotian era 535 million years ago and predates the rise of arthropods. The ancient origin and evolutionary persistence of Pv are clear indications that it has an important function.

In vertebrates, the sequential nature of the Vtg primary structure means that the Pv domains are covalently linked to the outer edges of the homodimeric Vtg structure between the LvH A-sheet and LvL domain [64, 69]. This arrangement allows the Pv domains to form loops that cover the large lipid cavities of the Vtg homodimer, permitting the inner hydrophobic backbone of the polyserine domain to interact with the lipids in the cavity, while the charged hydrophilic phosphates, which are attached to the Ser residues, interface with the solvent (Fig. 1). The Pv domains thus represent specialized amphipathic structures. This is in line with the β-sheet structure

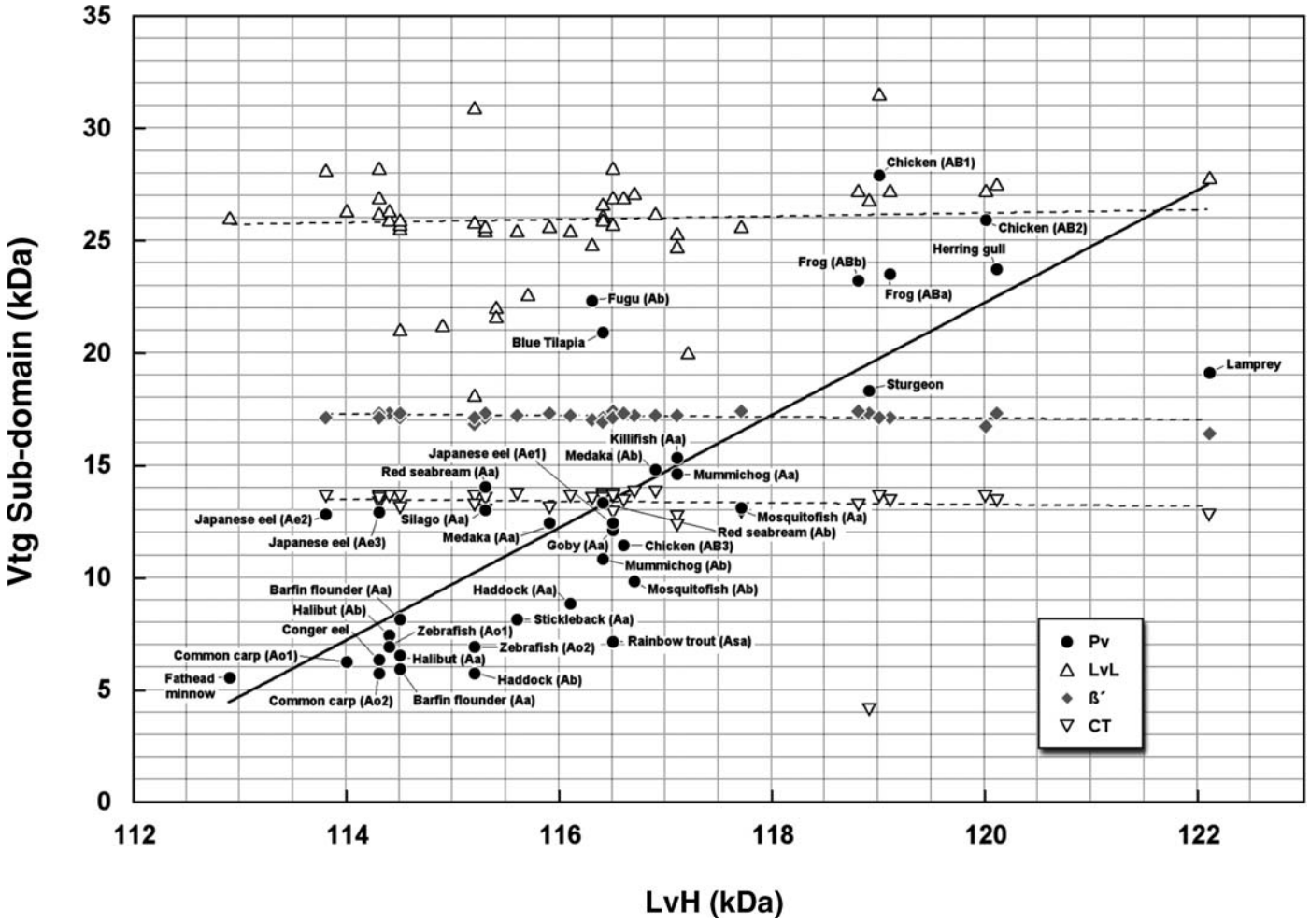

FIG. 4. Plot of predicted molecular masses of vitellogenin subdomains based on LvL-CS (Fig. 2) as a function of the predicted molecular mass of the lipovitellin heavy chain (LvH). Only phosvitins (Pv) have taxa labels and demonstrate a highly significant ($P < 0.005$) positive linear relationhip to LvH ($y = 2.502x - 278.08$; $r = 0.79$). The size of the lipovitellin light chain (LvL), beta′ components (β′) and C-terminal coding regions (CT) are highly conserved and independent of the predicted molecular mass of the LvH.

suggested for salmon egg Pv [70]. The basic amino acids, such as Arg and Lys in Atlantic halibut and His in other vertebrates, would further enhance solubility, while structural stability would be cemented following posttranslational phosphorylation of Ser residues and the subsequent binding of Ca^{2+}. It is also well-established that ApoB, which is a descendent of Vtg [6, 71–73], is synthesized cotranslationally in the liver [74, 75]. The loading of lipid is critical to the stability of the nascent lipoprotein [75–77]. However, ApoB does not have a polyserine domain but has a hairpin salt bridge [75, 78], so it relies on a related protein, microsomal triglyceride transfer protein (MTP), to deliver lipid to its folding core [77–81]. In the present context, it is proposed that Pv stabilizes the nascent Vtg while it receives its lipid cargo, and thus facilitates the hepatic loading and locking of lipid within the (C-sheet)-(A-sheet)-(LvL) cavity. Once Pv is phosphorylated in the Golgi complex, it enhances the solubility of the Vtg lipoprotein for secretion to the circulating plasma. It is further suggested that the stabilizing properties of Pv protect Vtg against premature degradation. The location of iPv1 in insects lies between the N-sheet and α-helical domain, where there is an opening to the lipid cavity (Fig. 1). Thus, iPv1, which is shorter than the vertebrate Pv, may perform the same primary function as that proposed above for vPv.

The size of the Pv domain is highly correlated to the size of the LvH domain (Fig. 4), which may indicate greater lipid-loading capacity associated with larger lipid pockets. However, the data in the literature for the lipid contents of vitellogenin and eggs do not support this notion [82]. An alternative possibility is a relationship between LvH-Pv size and the type of lipid in the egg. More than two thirds of the lipid transported by Vtg is phosphatidylcholine (PC), while neutral lipids (mainly triacylglycerols; TAG or wax esters) comprise the remainder [42, 64, 82–86]. Within both freshwater and marine teleosts, short Pv domains seem to be correlated with eggs that do not possess large oil globules, but rather have a preponderance of PC, as in Atlantic halibut [87]. However, the longer Pv domains mostly belong to species that have oil globules with a high content of neutral lipids. Therefore, Vtg may have a higher neutral lipid load in these latter species, and this would require larger amphipathic structures to maintain solubility in the plasma. Further studies are needed to clarify this notion. The strong correlation with the size of the LvH suggests that larger pockets may be necessary to accommodate neutral lipids. However, it is recognized that the Pv domain is not obligatory for lipid transport, since the phosvitinless class of Vtg (VtgC) does transport lipids, albeit at lower levels, i.e., 13.7% compared to 16–21% by mass in complete Vtgs [42, 82]. It is further recognized that most of the neutral lipid

delivered to oocytes that have large oil globules is not via Vtg but via other lipoproteins [88–90].

Another function of Pv is to bind Ca^{2+} and port P_i and metal ions into the oocyte. Either during passage in the blood or once in the oocyte, the Pv domains act as an acceptor for ferric iron (Fe^{3+}) [91], which is delivered separately by transferrin [92, 93]. This latter property of Pv may explain the novel observations of the role of Vtg in defense reactions [94]. Contrary to the suggestions of Shi et al. [94], Vtg is not related to the clotting proteins of crustaceans or echinoderms. The pacifastin of crayfish [95] and the Yps of echinodermata and cephalochordata are related to the transferrin family of proteins, and as such are important antimicrobial agents in the defense against pathogenic 'iron pirates' [92, 93].

A further function of Pv is expressed in pelagophil teleosts, such as the Atlantic halibut, wherein the secondary cleavage event during oocyte maturation results in dephosphorylation, and the released P_i contributes to the osmolyte pool that hydrates the oocyte [65]. Although the Pv-ported Ca^{2+} and P_i may eventually contribute to bone formation, cuticle or shell secretion, these functions are at the end of a long series of cell signaling events. Among other events, Ca^{2+} released from phosvitin during the acidification step in the early endosomes participates in the activation of SNARE protein-mediated membrane fusion of the endosomes [96–98], and is subsequently involved in the cortical reaction. The released P_i contributes to intracellular signaling through phosphorylation cascades, and after fertilization and the resumption of mitosis, it contributes to the adenylate pool. In this latter respect, P_i represents a vital substrate for nucleic acid synthesis in the blastulae prior to gastrulation and organogenesis, at which time-point the first ionoregulatory systems are established. Finally, both Ca^{2+} and P_i may contribute to other mineralization pools, although as stated, by this time the embryo has developed the ability to sequester minerals from external sources.

VON WILLEBRAND FACTOR

The β′ and CT domains in teleosts are the cleavage products of a larger protein that is homologous to VWFD [2, 3, 6, 99]. In other nonmammalian vertebrates, VWFD remains intact as YGP40 in chicken [100] but as in teleosts, it may not be incorporated into the yolk platelets. Since the major form of Vtg in zebrafish, VtgAo1 (previously reported as Vtg1 [41, 101]), is expressed at a 100-1000-fold higher level than other forms (VtgAo2 and VtgC [41]) but lacks the β′ and CT domains, it seems clear that β′, CT, and Vwfd are not involved in the yolk crystallization process. In zebrafish, the Yps are known to crystallize in an orthorhombic lattice [102].

The very high cysteine content of the Vwfd and its conservation throughout the metazoa implicate its functional importance. Its three dimensional location is predicted to lie between the α-helical domain and the C-sheet of the Vtg dimer (Fig. 1). In this locus, it protrudes into the solvent, and may thus aid solubility via its *N*-linked glycosyl component [100], while simultaneously stabilizing the dimer. Alternatively, it may play a role in cellular recognition, as suggested for mucins and zonadhesins (see below), and provide a point of anchor that facilitates the binding of Vtg to Vtgr. Once Vtg is internalized by the oocyte, the Vwfd is the only native component (26–33 kDa) that consistently separates from the rest of the Vtg dimer in both pelagophil and benthophil species [8, 9, 30, 38, 42–44, 103–105]. In humans, the precursor VWF molecule (pro-VWF) contains two RGD motifs: an RGDC motif in the N-terminal D2 domain, and an RGDS motif in the mature C-terminal C1 domain [106, 107]. These motifs interact with the exposed extracellular matrix via activated αIIbβ3 integrins in the endothelial walls [108], while the remaining segments of the VWF cause aggregation of platelets as part of the hemostatic clot cascade [109–111]. In other mammals and nonmammalian vertebrates, the RGD motifs are lacking [6, 112]. This suggests that the platelet-aggregating properties of VWF do not depend on the RGD motif but are instead induced by a shear force that transforms the VWF from a globular condensed conformation to an extended chain conformation [108]. The globular nature of VWF may explain its lubricant properties in mucins [113–115], while its extended conformation may explain its cell adhesive properties in other proteins, such as integrins and zonadhesins [108]. In the present context, the blood-clotting properties of the VWFD may have arisen from yolk platelet adhesion.

The higher expression levels of coagulation factor VIII when coexpressed with VWF are thought to be due to the proteolysis-protective properties of VWF [116]. This property may be important for the protection of Vtg during passage in the systemic circulation, as well as during the differential proteolysis of the Yps of marine teleosts during final oocyte maturation [5, 65]. However, the absence of the Vwfd in the major Vtgs expressed by Ostariophysian fishes [41, 45, 101, 117, 118] and in all VtgC forms suggests that other functional solutions have been realized among fish species. Furthermore, the proteolysis of the Vwfd domains during oocyte maturation in some marine pelagophil teleosts [5, 30, 44], as opposed to its persistence in other marine pelagophils ([105], Kolarevic and Finn, unpublished data) adds to the mystery surrounding the function of this protein. Further studies are necessary to elucidate these novel aspects of the subdomains of Vtg.

ACKNOWLEDGMENT

I am indebted to Hans Jørgen Fyhn for constructive criticism of the manuscript.

REFERENCES

1. Wallace RA. Vitellogenesis and oocyte growth in nonmammalian vertebrates. In: Browder LW (ed.), Developmental Biology, vol. 1. New York: Plenum Press; 1985:127–177.
2. Byrne BM, Gruber M, Ab G. The evolution of egg yolk proteins. Prog Biophys Mol Biol 1989; 53:33–69.
3. Chen JS, Sappington TW, Raikhel AS. Extensive sequence conservation among insect, nematode, and vertebrate vitellogenins reveals ancient common ancestry. J Mol Evol 1997; 44:440–451.
4. Sappington TW, Raikhel AS. Molecular characteristics of insect vitellogenins and vitellogenin receptors. Insect Biochem Mol Biol 1998; 28:277–300.
5. Finn RN. The maturational disassembly and differential proteolysis of paralogous vitellogenins in a marine pelagophil teleost: a conserved mechanism of oocyte hydration. Biol Reprod 2002; 76:936–948.
6. Finn RN, Kristoffersen BA. Vertebrate vitellogenin gene duplication in relation to the "3R Hypothesis": correlation to the pelagic egg and the oceanic radiation of teleosts. PLoS ONE 2007; 2:e169.
7. Mosconi G, Carnevali O, Habibi HR, Sanyal R, Polzonetti-Magni AM. Hormonal mechanisms regulating hepatic vitellogenin synthesis in the gilthead seabream, *Sparus aurata*. Am J Physiol Cell Physiol 2002; 283: 673–678.
8. Jared DW, Wallace RA. Comparative chromatography of the yolk proteins of teleosts. Comp Biochem Physiol 1968; 24:437–443.
9. Markert JR, Vanstone WE. Egg proteins of coho salmon (*Oncorhynchus kisutch*): chromatographic separation and molecular weights of the major proteins in the high density fraction and their presence in salmon plasma. J Fish Res Bd Can 1971; 28:1853–1856.
10. Wallace RA, Selman K. Ultrastructural aspects of oogenesis and oocyte growth in fish and amphibians. J Electron Microsc Tech 1990; 16:175–201.

11. Conner SD, Schmid SL. Regulated portals of entry into the cell. Nature 2003; 422:37–44.
12. Sorkin A. Cargo recognition during clathrin-mediated endocytosis: a team effort. Curr Opin Cell Biol 2004; 16:392–399.
13. Duncan MC, Payne GS. Cell biology: protein choreography. Nature 2005; 438:571–573.
14. Clague MJ, Hammond DE. Membrane traffic: catching the lysosome express. Curr Biol 2006; 16:R416–418.
15. Lakadamyali M, Rust MJ, Zhuang X. Ligands for clathrin-mediated endocytosis are differentially sorted into distinct populations of early endosomes. Cell 2006; 124:997–1009.
16. Busson-Mabillot S. Endosomes transfer yolk proteins to lysosomes in the vitellogenic oocyte of the trout. Biol Cell 1984; 51:53–66.
17. Fagotto F. Regulation of yolk degradation, or how to make sleepy lysosomes. J Cell Sci 1995; 108:3645–3647.
18. Selman K, Wallace RA, Cerdà J. Bafilomycin A1 inhibits proteolytic cleavage and hydration but not yolk crystal disassembly or meiosis during maturation of sea bass oocytes. J Exp Zool 2001; 290:265–278.
19. Raldúa D, Fabra M, Bozzo MG, Weber E, Cerdà J. Cathepsin B-mediated yolk protein degradation during killifish oocyte maturation is blocked by an H^+-ATPase inhibitor: effects on the hydration mechanism. Am J Physiol Regul Integr Comp Physiol 2006; 290:R456–466.
20. Yoshizaki N, Yonezawa S. Cathepsin D activity in the vitellogenesis of *Xenopus laevis*. Dev Growth Differ 1994; 36:299–306.
21. Hiramatsu N, Hara A. Specific proteolysis of vitellogenin to egg yolk proteins in white spotted-charr *Salvelinus leucomaenis*. Nippon Suisan Gakkaishi 1997; 63:701–708.
22. Carnevali O, Carletta R, Cambi A, Vita A, Bromage N. Yolk formation and degradation during oocyte maturation in seabream *Sparus aurata*: involvement of two lysosomal proteinases. Biol Reprod 1999; 60:140–146.
23. Carnevali O, Cionna C, Tosti L, Lubzens E, Maradonna F. Role of cathepsins in ovarian follicle growth and maturation. Gen Comp Endocrinol 2006; 146:195–203.
24. Hiramatsu N, Ichikawa N, Fukada H, Fujita T, Sullivan CV, Hara A. Identification and characterization of proteases involved in specific proteolysis of vitellogenin and yolk proteins in salmonids. J Exp Zool 2002; 292:11–25.
25. Fabra M, Cerdà J. Ovarian cysteine proteinases in the teleost Fundulus heteroclitus: molecular cloning and gene expression during vitellogenesis and oocyte maturation. Mol Reprod Dev S 2004; 67:282–294.
26. Romano M, Rosanova P, Anteo C, Limatola E. Vertebrate yolk proteins: a review. Mol Reprod Dev 2004; 69:109–116.
27. Hiramatsu N, Cheek AO, Sullivan CV, Matsubara T, Hara A. Vitellogenesis and endocrine disruption. In: Mommsen TP, Moon TW (eds.), Biochemistry and Molecular Biology of Fishes, vol. 6. Amsterdam: Elsevier Science BV; 2006:431–471.
28. LaFleur GJ Jr, Byrne BM, Kanungo J, Nelson LD, Greenberg RM, Wallace RA. *Fundulus heteroclitus* vitellogenin: the deduced primary structure of a piscine precursor to noncrystalline, liquid-phase yolk protein. J Mol Evol 1995; 41:505–521.
29. LaFleur GJ Jr, Raldúa D, Fabra M, Carnevali O, Denslow N, Wallace RA, Cerdà J. Derivation of major yolk proteins from parental vitellogenins and alternative processing during oocyte maturation in *Fundulus heteroclitus*. Biol Reprod 2005; 73:815–824.
30. Matsubara T, Ohkubo N, Andoh T, Sullivan CV, Hara A. Two forms of vitellogenin, yielding two distinct lipovitellins, play different roles during oocyte maturation and early development of barfin flounder, *Verasper moseri*, a marine teleost that spawns pelagic eggs. Dev Biol 1999; 213: 18–32.
31. Matsubara T, Nagae M, Ohkubo N, Andoh T, Sawaguchi S, Hiramatsu N, Sullivan CV, Hara A. Multiple vitellogenins and their unique roles in marine teleosts. Fish Physiol Biochem 2003; 28:295–299.
32. Trichet V, Buisine N, Mouchel N, Moran P, Pendas AM, Le Pennec JP, Wolff J. Genomic analysis of the vitellogenin locus in rainbow trout (*Oncorhynchus mykiss*) reveals a complex history of gene amplification and retroposon activity. Mol Gen Genet S 2000; 263:828–837.
33. Reith M, Munholland J, Kelly J, Finn RN, Fyhn HJ. Lipovitellins derived from two forms of vitellogenin are differentially processed during oocyte maturation in haddock (*Melanogrammus aeglefinus*). J Exp Zool 2001; 291:58–67.
34. Buisine N, Trichet V, Wolff J. Complex evolution of vitellogenin genes in salmonid fishes. Mol Genet Genomics 2002; 268:535–542.
35. Hiramatsu N, Matsubara T, Hara A, Donato DM, Hiramatsu K, Denslow ND, Sullivan CV. Identification, purification and classification of multiple forms of vitellogenin from white perch (*Morone americana*). Fish Physiol Biochem 2002; 26:355–370.
36. Hiramatsu N, Hara A, Matsubara T, Hiramatsu K, Sullivan CV. Oocyte growth in temperate basses: multiple forms of vitellogenin and their receptor. Fish Physiol Biochem 2003; 28:301–303.
37. Ohkubo N, Mochida K, Adachi S, Hara A, Hotta K, Nakamura Y, Matsubara T. Development of enzyme-linked immunosorbent assays for two forms of vitellogenin in Japanese common goby (*Acanthogobius flavimanus*). Gen Comp Endocrinol 2003; 131:353–364.
38. Ohkubo N, Andoh T, Mochida K, Adachi S, Hara A, Matsubara T. Deduced primary structure of two forms of vitellogenin in Japanese common goby (*Acanthogobius flavimanus*). Gen Comp Endocrinol 2004; 137:19–28.
39. Cohen AM, Mansour AA, Banoub JH. '*De novo*' sequencing of Atlantic cod vitellogenin tryptic peptides by matrix-assisted laser desorption/ionization quadrupole time-of-flight tandem mass spectrometry: similarities with haddock vitellogenin. Rapid Commun Mass Spectrom 2005; 19:2454–2460.
40. Fujiwara Y, Fukada H, Shimizu M, Hara A. Purification of two lipovitellins and development of immunoassays for two forms of their precursors (vitellogenins) in medaka (*Oryzias latipes*). Gen Comp Endocrinol 2005; 143:267–277.
41. Wang H, Tan JT, Emelyanov A, Korzh V, Gong Z. Hepatic and extrahepatic expression of vitellogenin genes in the zebrafish, *Danio rerio*. Gene 2005; 356:91–100.
42. Sawaguchi S, Koya Y, Yoshizaki N, Ohkubo N, Andoh T, Hiramatsu N, Sullivan CV, Hara A, Matsubara T. Multiple vitellogenins (Vgs) in mosquitofish (*Gambusia affinis*): identification and characterization of three functional Vg genes and their circulating and yolk protein products. Biol Reprod 2005; 72:1045–1060.
43. Sawaguchi S, Ohkubo N, Koya Y, Matsubara T. Incorporation and utilization of multiple forms of vitellogenin and their derivative yolk proteins during vitellogenesis and embryonic development in the mosquitofish, *Gambusia affinis*. Zool Sci 2005; 22:701–710.
44. Sawaguchi S, Kagawa H, Ohkubo N, Hiramatsu N, Sullivan CV, Matsubara T. Molecular characterization of three forms of vitellogenin and their yolk protein products during oocyte growth and maturation in red seabream (*Pagrus major*), a marine teleost spawning pelagic eggs. Mol Reprod Dev 2006; 73:719–736.
45. Miracle A, Ankley G, Lattier D. Expression of two vitellogenin genes (vg1 and vg3) in fathead minnow (*Pimephales promelas*) liver in response to exposure to steroidal estrogens and androgens. Ecotoxicol Environ Saf 2006; 63:337–342.
46. Ohlendorf DH, Barbarash GR, Trout A, Kent C, Banaszak LJ. Lipid and polypepide components of the crystalline yolk system from *Xenopus laevis*. J Biol Chem 1997; 252:7992–8001.
47. Yoshitome S, Nakamura H, Nakajo N, Okamoto K, Sugimoto I, Kohara H, Kitayama K, Igarashi K, Ito S, Sagata N, Hashimoto E. Mr 25 000 protein, a substrate for protein serine/threonine kinases, is identified as a part of *Xenopus laevis* vitellogenin B1. Dev Growth Differ 2003; 45: 283–294.
48. Bergink EW, Wallace RA. Precursor-product relationship between amphibian vitellogenin and the yolk proteins, lipovitellin and phosvitin. J Biol Chem 1974; 249:2897–2903.
49. Wallace RA, Hoch KL, Carnevali O. Placement of small lipovitellin subunits within the vitellogenin precursor in *Xenopus laevis*. J Mol Biol 1990; 213:407–409.
50. Gerber-Huber S, Nardelli D, Haefliger JA, Cooper DN, Givel F, Germond JE, Engel J, Green NM, Wahli W. Precursor-product relationship between vitellogenin and the yolk proteins as derived from the complete sequence of a *Xenopus* vitellogenin gene. Nucleic Acids Res 1987; 15:4737–4760.
51. Wang SY, Williams DL. Identificiation, purification, and characterization of two distinct avian vitellogenins. Biochemistry 1980; 19:1557–1563.
52. Wang SY, Smith DE, Williams DL. Purification of avian vitellogenin III: comparison with vitellogenins I and II. Biochemistry 1983; 22:6206–6212.
53. van het Schip FD, Samallo J, Broos J, Ophuis J, Mojet M, Gruber M, Ab G. Nucleotide sequence of a chicken vitellogenin gene and derived amino acid sequence of the encoded yolk precursor protein. J Mol Biol 1987; 196:245–260.
54. Silva R, Fischer AH, Burch JB. The major and minor chicken vitellogenin genes are each adjacent to partially deleted pseudogene copies of the other. Mol Cell Biol 1989; 9:3557–3562.
55. Wiley HS, Wallace RA. The structure of vitellogenin. Multiple vitellogenins in *Xenopus laevis* give rise to multiple forms of the yolk proteins. J Biol Chem 1981; 256:8626–8634.
56. Byrne BM, van het Schip AD, van de Klundert JA, Arnberg AC, Gruber M, Ab G. Amino acid sequence of phosvitin derived from the nucleotide

sequence of part of the chicken vitellogenin gene. Biochemistry 1984; 23:4275–4279.
57. Wallace RA, Morgan JP. Chromatographic resolution of chicken phosvitin. Multiple macromolecular species in a classic vitellogenin-derived phosphoprotein. Biochem J 1986; 240:871–878.
58. Wallace RA, Morgan JP. Isolation of phosvitin: retention of small molecular weight species and staining characteristics on electrophoretic gels. Anal Biochem 1986; 157:256–261.
59. Elkin RG, Freed MB, Danetz SA, Bidwell CA. Proteolysis of Japanese quail and chicken plasma apolipoprotein B and vitellogenin by cathepsin D: similarity of the resulting protein fragments with egg yolk polypeptides. Comp Biochem Physiol B Biochem Mol Biol 1995; 112: 191–196.
60. Castellani O, Martinet V, David-Briand E, Guerin-Dubiard C, Anton M. Egg yolk phosvitin: preparation of metal-free purified protein by fast protein liquid chromatography using aqueous solvents. J Chromatogr B Analyt Technol Biomed Life Sci 2003; 791:273–284.
61. Clark RC. The primary structure of avian phosvitins. Contributions through the Edman degradation of methylmercaptovitins prepared from the constituent phosphoproteins. Int J Biochem 1985; 17:983–988.
62. Groche D, Rashkovetsky LG, Falchuk KH, Auld DS. Subunit composition of the zinc proteins alpha- and beta-lipovitellin from chicken. J Protein Chem 2000; 19:379–387.
63. Johanning KM, Specker JL. Characterization of yolk proteins during oocyte development of tilapia, *Oreochromis mossambicus*. Comp Biochem Physiol 1995; 112B:177–189.
64. Anderson TA, Levitt DG, Banaszak LJ. The structural basis of lipid interactions in lipovitellin, a soluble lipoprotein. Structure 1998; 6:895–909.
65. Finn RN, Ostby GC, Norberg B, Fyhn HJ. *In vivo* oocyte hydration in Atlantic halibut (*Hippoglossus hippoglossus*); proteolytic liberation of free amino acids, and ion transport, are driving forces for osmotic water influx. J Exp Biol 2002; 205:211–224.
66. Sharrock WJ, Rosenwasser TA, Gould J, Knott J, Hussey D, Gordon JI, Banaszak L. Sequence of lamprey vitellogenin. Implications for the lipovitellin crystal structure. J Mol Biol 1992; 226:903–907.
67. Lim EH, Teo BY, Lam TJ, Ding JL. Sequence analysis of a fish vitellogenin cDNA with a large phosvitin domain. Gene 2001; 277:175–186.
68. Chen JS, Cho WL, Raikhel AS. Analysis of mosquito vitellogenin cDNA. Similarity with vertebrate phosvitins and arthropod serum proteins. J Mol Biol 1994; 237:641–647.
69. Thompson JR, Banaszak LJ. Lipid-protein interactions in lipovitellin. Biochemistry 2002; 41:9398–9409.
70. Losso JN, Bogumil R, Nakai S. Comparative studies of phosvitin from chicken and salmon egg yolk. Comp Biochem Physiol B 1993; 106:919–923.
71. Baker ME. Is vitellogenin an ancestor of apolipoprotein B-100 of human low-density lipoprotein and human lipoprotein lipase? Biochem J 1988; 255:1057–1060.
72. Babin PJ, Bogerd J, Kooiman FP, Van Marrewijk WJ, Van der Horst DJ. Apolipophorin II/I, apolipoprotein B, vitellogenin, and microsomal triglyceride transfer protein genes are derived from a common ancestor. J Mol Evol 1999; 49:150–160.
73. Perez LE, Fenton MJ, Callard IP. Vitellogenin-homologs of mammalian apolipoproteins? Comp Biochem Physiol B 1991; 100:821–826.
74. Davis RA. Evolution of processes and regulators of lipoprotein synthesis: from birds to mammals. J Nutr 1997; 127:795S–800S.
75. Richardson PE, Manchekar M, Dashti N, Jones MK, Beigneux A, Young SG, Harvey SC, Segrest JP. Assembly of lipoprotein particles containing apolipoprotein-B: structural model for the nascent lipoprotein particle. Biophys J 2005; 88:2789–2800.
76. Jiang ZG, Carraway M, McKnight CJ. Limited proteolysis and biophysical characterization of the lipovitellin homology region in apolipoprotein B. Biochemistry 2005; 44:1163–1173.
77. Manchekar M, Richardson PE, Forte TM, Datta G, Segrest JP, Dashti N. Apolipoprotein B-containing lipoprotein particle assembly: lipid capacity of the nascent lipoprotein particle. J Biol Chem 2004; 279:39757–39766.
78. Dashti N, Gandhi M, Liu X, Lin X, Segrest JP. The N-terminal 1000 residues of apolipoprotein B associate with microsomal triglyceride transfer protein to create a lipid transfer pocket required for lipoprotein assembly. Biochemistry 2002; 41:6978–6987.
79. Mann CJ, Anderson TA, Read J, Chester SA, Harrison GB, Kochl S, Ritchie PJ, Bradbury P, Hussain FS, Amey J, Vanloo B, Rosseneu M, et al. The structure of vitellogenin provides a molecular model for the assembly and secretion of atherogenic lipoproteins. J Mol Biol 1999; 285:391–408.
80. Segrest JP, Jones MK, Dashti N. N-terminal domain of apolipoprotein B has structural homology to lipovitellin and microsomal triglyceride transfer protein: a "lipid pocket" model for self-assembly of apob-containing lipoprotein particles. J Lipid Res 1999; 40:1401–1416.
81. Segrest JP, Jones MK, De Loof H, Dashti N. Structure of apolipoprotein B-100 in low density lipoproteins. J Lipid Res 2001; 42:1346–1367.
82. Silversand C. Vitellogenesis in teleost fish. A study of vitellogenin and egg lipids. Göteborg, Sweden: University of Göteborg; 1996. Thesis.
83. Norberg B, Haux C. Induction, isolation and a characterization of the lipid content of plasma vitellogenin from two Salmo species: rainbow trout (*Salmo gairdneri*) and sea trout (*Salmo trutta*). Comp Biochem Physiol B 1985; 81:869–876.
84. Finn RN, Fyhn HJ, Henderson RJ, Evjen MS. The sequence of catabolic substrate oxidation and enthalpy balance of developing embryos and yolk-sac larvae of turbot (*Scophthalmus maximus* L.). Comp Biochem Physiol 1996; 115A:133–151.
85. Ohkubo N, Matsubara T. Sequential utilization of free amino acids, yolk proteins and lipids in developing eggs and yolk-sac larvae of barfin flounder *Verasper moseri*. Mar Biol 2002; 140:187–196.
86. Ohkubo N, Sawaguchi S, Hamatsu T, Matsubara T. Utilization of free amino acids, yolk proteins and lipids in developing eggs and yolk-sac larvae of walleye pollock *Theragra chalcogramma*. Fish Sci 2006; 76: 620–630.
87. Rønnestad I, Finn RN, Lein I, Lie Ø. Compartmental changes in total lipid, lipid classes and their associated fatty acids of developing yolk-sac larvae of Atlantic halibut (*Hippoglossus hippoglossus* L.). Aquaculture Nutrition 1995; 1:119–130.
88. Kwon JY, Prat F, Randall C, Tyler CR. Molecular characterization of putative yolk processing enzymes and their expression during oogenesis and embryogenesis in rainbow trout (*Oncorhynchus mykiss*). Biol Reprod 2001; 65:1701–1709.
89. Ibañez AJ, Peinado-Onsurbe J, Sanchez E, Prat F. The role of lipoprotein lipase (LPL) in the incorporation of neutral lipids into the oocytes of the European sea bass (*Dicentrarchus labrax* L.) during gonadal development. Fish Physiol Biochem 2003; 28:291–293.
90. Albalat A, Sanchez-Gurmaches J, Gutierrez J, Navarro I. Regulation of lipoprotein lipase activity in rainbow trout (*Oncorhynchus mykiss*) tissues. Gen Comp Endocrinol 2006; 146:226–235.
91. Grogan J, Taborsky G. Iron binding by phosvitins: variable mechanism of iron release by phosvitins of diverse species characterized by different degrees of phosphorylation. J Inorg Biochem 1987; 29:33–47.
92. Lambert LA, Perri H, Meehan TJ. Evolution of duplications in the transferrin family of proteins. Comp Biochem Physiol B Biochem Mol Biol 2005; 140:11–25.
93. Lambert LA, Perri H, Halbrooks PJ, Mason AB. Evolution of the transferrin family: conservation of residues associated with iron and anion binding. Comp Biochem Physiol B Biochem Mol Biol 2005; 142: 129–141.
94. Shi X, Zhang S, Pang Q. Vitellogenin is a novel player in defense reactions. Fish Shellfish Immunol 2006; 20:769–772.
95. Liang Z, Sottrup-Jensen L, Aspan A, Hall M, Soderhall K. Pacifastin, a novel 155-kDa heterodimeric proteinase inhibitor containing a unique transferrin chain. Proc Natl Acad Sci U S A 1997; 94:6682–6687.
96. Sutton RB, Fasshauer D, Jahn R, Brunger AT. Crystal structure of a SNARE complex involved in synaptic exocytosis at 2.4 Å resolution. Nature 1998; 395:347–353.
97. Reese C, Heise F, Mayer A. Trans-SNARE pairing can precede a hemifusion intermediate in intracellular membrane fusion. Nature 2005; 436:410–414.
98. Leabu M. Membrane fusion in cells: molecular machinery and mechanisms. J Cell Mol Med 2006; 10:423–427.
99. Baker ME. Invertebrate vitellogenin is homologous to human von Willebrand factor. Biochem J 1988; 256:1059–1061.
100. Yamamura J, Adachi T, Aoki N, Nakajima H, Nakamura R, Matsuda T. Precursor-product relationship between chicken vitellogenin and the yolk proteins: the 40 kDa yolk plasma glycoprotein is derived from the C-terminal cysteine-rich domain of vitellogenin II. Biochim Biophys Acta 1995; 1244:384–394.
101. Wang H, Yan T, Tan JT, Gong Z. A zebrafish vitellogenin gene (vg3) encodes a novel vitellogenin without a phosvitin domain and may represent a primitive vertebrate vitellogenin gene. Gene 2000; 256:303–310.
102. Selman K, Wallace RA, Sarka A, Qi X. Stages of oocyte development in the zebrafish *Brachydanio rerio*. J Morphol 1993; 218:203–224.
103. Campbell CM, Idler DR. Characterization of an estradiol-induced protein from rainbow trout serum as vitellogenin by the composition and

radioimmunological cross reactivity to ovarian yolk fractions. Biol Reprod 1980; 22:605–617.
104. Riazi A, Fremont L, Gozzelino MT. Characterization of egg yolk proteins from rainbow trout *Salmo gairdneri* (Rich.). Comp Biochem Physiol 1988; 89B:399–407.
105. Hiramatsu N, Matsubara T, Weber GM, Sullivan CV, Hara A. Vitellogenesis in aquatic animals. Fish Sci 2002; 68:694–699.
106. Sadler JE, Shelton-Inloes BB, Sorace JM, Harlan JM, Titani K, Davie EW. Cloning and characterization of two cDNAs coding for human von Willebrand factor. Proc Natl Acad Sci U S A 1985; 82:6394–6398.
107. Verweij CL, Diergaarde PJ, Hart M, Pannekoek H. Full-length von Willebrand factor (vWF) cDNA encodes a highly repetitive protein considerably larger than the mature vWF subunit. EMBO J 1986; 5: 1839–1847.
108. Sadler JE. Biochemistry and genetics of von Willebrand factor. Annu Rev Biochem 1998; 67:395–424.
109. Pierschbacher MD, Ruoslahti E. Cell attachment activity of fibronectin can be duplicated by small synthetic fragments of the molecule. Nature 1984; 309:30–33.
110. Pierschbacher MD, Hayman EG, Ruoslahti E. The cell attachment determinant in fibronectin. J Cell Biochem 1985; 28:115–126.
111. Michaux G, Abbitt KB, Collinson LM, Haberichter SL, Norman KE, Cutler DF. The physiological function of von Willebrand's factor depends on its tubular storage in endothelial Weibel-Palade bodies. Dev Cell 2006; 10:223–232.
112. Janel N, Ribba AS, Cherel G, Kerbiriou-Nabias D, Meyer D. Primary structure of the propeptide and factor VIII-binding domain of bovine von Willebrand factor. Biochim Biophys Acta 1997; 1339:4–8.
113. Desseyn JL, Aubert JP, Van Seuningen I, Porchet N, Laine A. Genomic organization of the 3' region of the human mucin gene MUC5B. J Biol Chem 1997; 272:16873–16883.
114. Gipson IK, Ho SB, Spurr-Michaud SJ, Tisdale AS, Zhan Q, Torlakovic E, Pudney J, Anderson DJ, Toribara NW, Hill JA III. Mucin genes expressed by human female reproductive tract epithelia. Biol Reprod 1997; 56:999–1011.
115. Toribara NW, Ho SB, Gum E, Gum JRJ, Lau P, Kim YS. The carboxyl-terminal sequence of the human secretory mucin, MUC6. Analysis of the primary amino acid sequence. J Biol Chem 1997; 272:16398–16403.
116. Chen C, Fang JX, Zhu J, Wu XF, Zhang ZC, Gu JX, Wang ZY, Chi CW. The gene expression of coagulation factor VIII in mammalian cell lines. Thromb Res 1999; 95:105–115.
117. Fukada H, Fujiwara Y, Takahashi T, Hiramatsu N, Sullivan CV, Hara A. Carp (*Cyprinus carpio*) vitellogenin: purification and development of a simultaneous chemiluminescent immunoassay. Comp Biochem Physiol A Mol Integr Physiol 2003; 134:615–623.
118. Hennies M, Wiesmann M, Allner B, Sauerwein H. Vitellogenin in carp (*Cyprinus carpio*) and perch (*Perca fluviatilis*): purification, characterization and development of an ELISA for the detection of estrogenic effects. Sci Total Environ 2003; 309:93–103.
119. Chen J, Anderson JB, DeWeese-Scott C, Fedorova ND, Geer LY, He S, Hurwitz DI, Jackson JD, Jacobs AR, Lanczycki CJ, Liebert CA, Liu C, et al. MMDB: Entrez's 3D-structure database. Nucleic Acids Res 2003; 31: 474–477.
120. Li A, Sadasivam M, Ding JL. Receptor-ligand interaction between vitellogenin receptor (VtgR) and vitellogenin (Vtg), implications on low density lipoprotein receptor and apolipoprotein B/E. The first three ligand-binding repeats of VtgR interact with the amino-terminal region of Vtg. J Biol Chem 2003; 278:2799–2806.